# Cloud-Layer Overlap Characteristics Derived from Long-Term Cloud Radar Data

GERALD G. MACE AND SALLY BENSON-TROTH

*Department of Meteorology, University Of Utah, Salt Lake City, Utah*

(Manuscript received 19 November 2001, in final form 15 February 2002)

ABSTRACT

Assumptions regarding the vertical overlap characteristics of horizontal cloudy layers have been shown to be important to both the radiation transfer and the cloud microphysics that are predicted in general circulation models. Certain reasonable assumptions regarding cloud-layer overlap have been applied in models up to now where vertically continuous cloudy layers were assumed to overlap maximally leading to a minimum in cloud cover, and layers separated by noncloudy layers were assumed to overlap randomly. However, these assumptions have not been systematically evaluated with a comprehensive dataset that can resolve simultaneously occurring cloud layers. Presented here is an analysis of cloud-layer overlap characteristics derived from 103 months of cloud radar data collected by continuously operating millimeter-wavelength instruments deployed at the Atmospheric Radiation Measurement (ARM) sites in the Tropics, middle latitudes, and the Arctic. Using an approach recently proposed by Hogan and Illingworth, it is shown that an assumption of random overlap for layers separated by noncloudy layers is supported by observations. However, that the overlap characteristics of vertically continuous layers cannot be considered maximal is also shown. Indeed, vertically continuous cloudy layers do not appear to lend themselves to a simple overlap assumption. Therefore, to avoid significant biases in diagnosed cloud cover, the overlap properties of these layers in models will need to be parameterized. It is shown that the cloud-layer overlap characteristics in the middle latitudes do appear to be a strong function of season, suggesting that an overlap parameterization in terms of cloud system type may be possible.

## 1. Introduction

The representation of cloud cover[1] in numerical models has long been recognized as a potential source of uncertainty in climate predictions (Weatherald and Manabe 1988; Houghton et al. 1990). This uncertainty stems from difficulties associated with diagnosing fractional cloud cover within a grid box (Yao and Del Genio 1999; Slingo 1987) to the manner in which fractional cloud cover diagnosed or predicted at the model's vertical levels should overlap in the vertical dimension. The implications for the radiation budget due to assumptions regarding cloud overlap are clear and substantial. Consider, for instance, a 33% fractional cloud cover in each of three model layers distributed vertically with maximal overlap resulting in a total cloud cover fraction of 33%, to the overcast situation that would result if the cloud cover in these layers were minimally overlapped. Barker et al. (1999) succinctly illustrates the influence these assumptions have on the modeled solar flux in a tropical convective environment. Among other impacts, they show that by using widely accepted assumptions regarding cloud overlap, bias errors in solar reflection can easily exceed several hundred W $m^{-2}$.

Our day-to-day experience suggests that the actual overlap of cloud layers is a strong function of the cloud spatial scale, cloud type, and synoptic situation. For instance, cumulus clouds often appear vertically continuous as they develop into thunderstorms, while observers of midlatitude weather systems are familiar with the cloudiness associated with fronts that often progress from high-level cirrus to deepening alto- and nimbostratus. These intuitive observations regarding cloud overlap are largely substantiated by the few cloud contingency climatologies that have been published. For instance, Hahn et al. (1982) report that in boreal winter, the probability of observing altostratus and altocumulus, given the occurrence of stratus or stratocumulus, is approximately 60% along the northern storm tracks and southern oceans. During boreal summer, the probability of finding no other cloud types present when cumulus are observed ranges from a high of 70% in the trade wind zones of the subtropical high pressure regions to a low of approximately 30% in the northern oceans. It takes only a cursory examination of Hahn et al.'s con-

[1] Cloud cover is defined as the fractional area of a model grid box at a model level that is considered to be cloud filled. Some models (Yao and Del Genio 1999) extend this concept to a grid volume instead of just horizontal area.

*Corresponding author address:* Dr. Gerald Mace, Department of Meteorology, University of Utah, 135 South 1450 East, Rm 819 (819 WBB), Salt Lake City, UT 84112-0110.
E-mail: mace@met.utah.edu

tingency diagrams to see other patterns that are clearly related to seasonally dependent synoptic regimes.

Because global models attempt to represent processes within grid columns that have horizontal dimensions ranging from tens to hundreds of kilometers on a side, the overlap assumptions applied to cloud layers within a particular model should likely also be parameterized as a function of the model's resolved scale. Consider a frontal system that fits within the grid resolution of a coarse domain model compared to the same frontal system represented by a model with much higher horizontal resolution. In the coarse model, an assumption of minimal overlap would be needed to account for the sloping nature of the frontal system, while for the higher resolution model it might be more correct to assume maximal overlap. In addition to the radiation budget, correctly characterizing the overlap is necessary to faithfully model the evolution of the layer microphysics and precipitation. Jakob and Klein (1999) quantify this effect by using the European Centre for Medium-Range Weather Forecasts (ECMWF) model as a diagnostic tool. However, no climate model of which we are aware considers either synoptic regime or model resolution as a factor in its cloud overlap assumption. We can identify two primary reasons for this neglect of the cloud overlap assumption. As pointed out by Morcrette and Jakob (2000), traditional assumptions regarding cloud overlap are encoded deep within the radiation parameterizations of large-scale models where evaluation or adjustment requires substantial effort. More importantly, however, a dearth of definitive observational data have been available with which a thorough assessment of the overlap assumption could be made. Our purpose in this paper is to begin filling the observational gap.

Aside from the early climatologies of Hahn et al. (1982) and Warren et al. (1986), in which surface observer records that included only three vertical levels were evaluated, Tian and Curry (1989, hereafter TC89) were the first to quantitatively examine the cloud overlap problem with a reasonably comprehensive dataset. Using the 15-level U.S. Air Force 3D Nephanalysis (3DNEPH) product from January 1979 (Fye 1978) over the North Atlantic Ocean, they essentially validate the assumptions proposed by Geleyn and Hollingsworth (1979)—that cloud-layer overlap in adjacent model grid levels can be considered maximally overlapped, while cloud layers that are separated by interstices of clear air can be assumed to overlap randomly. TC89 did demonstrate that for larger grid sizes ($>$ 45-km square), the random overlap assumption tends to underestimate the total cloud fraction, suggesting a tendency toward minimal overlap for larger grid boxes containing discrete cloud layers. The dataset used by TC89, while spatially extensive, did, however, include implicit assumptions regarding random cloud overlap and the emissivity of cloud layers. While the 3DNEPH product tended to appear realistic, a systematic validation of the product was not possible over the data-sparse regions of their analysis domain.

The use of passive satellite data to evaluate cloud overlap suffers from the distinct disadvantage of not being able to sense the occurrence of cloud layers below any optically thick higher layer. As pointed out by Tian and Curry (1989), this would tend to bias their results toward the random overlap assumption. Surface-based millimeter radar (Kropfli et al. 1995; Clothiaux et al. 1995) has the unique ability, on the other hand, to sense hydrometeor occurrence through the depth of the troposphere regardless of the number of layers or the optical opacity of most nonprecipitating clouds. Moderate to heavy liquid precipitation can attenuate the radar beam completely, and in most cases very thin cirrus layers (visible optical depth less than approximately 0.25) can not be sensed by millimeter radar at all. The obvious disadvantage of vertically pointing ground-based millimeter radars compared to satellite imagery is the lack of an observed horizontal dimension. A standard assumption that is applied to such remote sensor time series, however, is an implicit conversion between time and space based on the advection of an airmass over the radar. Several investigators have used this assumption to their advantage in comparing millimeter radar data to model cloud predictions (Mace et al. 1998), while others have evaluated the decorrelation scales between time series data and spatial quantities (Barnett et al. 1998; Long and Ackerman 1995) and shown that these assumptions are reasonable, if applied carefully. Recently, Hogan and Illingworth (2000, hereafter HI00) used millimeter radar data collected over southern England between November 1998 and January 1999 to evaluate the overlap of cloud layers observed there. They introduced an innovative technique that we adopt and describe below, which essentially quantifies the overlap characteristics of cloud layers in vertically pointing active sensor data. HI00 found, counter to TC89, that vertically continuous cloudy layers tend toward random overlap with increasing vertical separation that had an *e*-folding distance dependent on temporal and vertical resolution. This *e*-folding distance ($\Delta z_0$) ranged from 1.4 km for 20-min temporal and 360-m vertical resolution to 2.93 km for 3 h and 1440-m resolution. Like TC89, they found that cloud layers separated by clear interstices could be modeled with an assumption of random overlap.

In this paper, we build on the work of these earlier observational studies and present cloud overlap results for the first time from an extensive cloud radar dataset collected at the Atmospheric Radiation Measurement (ARM) sites (Stokes and Schwartz 1994). This ARM millimeter radar dataset extends over multiple years and at four sites in three distinctly different climatic domains. As such, the ARM millimeter radar data represent the most comprehensive record of cloud-layer occurrence that has to date been collected from ground-based remote sensors. Exploring the full breadth of

TABLE 1. Specifics on the radar data examined in this paper including location (north latitude and west longitude are positive), date the radar system became operational, and the period we examine for cloud overlap. SGP refers to southern Great Plains, NSA to North Slope of Alaska, and TWP to the tropical western Pacific. The C1 and C2 designations are used to distinguish the two tropical locations described in the text.

| Location | Lat (°N) | Lon (°W) | Operational date | Period under study |
|---|---|---|---|---|
| SGP | 36.605 | 97.485 | Nov 1996 | Mar 1997–Dec 2000 (45 months) |
| NSA | 71.317 | 156.604 | May 1999 | Jan 1999–Dec 2000 (24 months) |
| TWP C1 | −2.058 | −147.425 | Jun 1999 | Jun 1999–Oct 2000 (14 months) |
| TWP C2 | −0.521 | −166.916 | Nov 1998 | Jan 1999–Oct 2000 (22 months) |

cloud-layer overlap information recorded in this dataset is well beyond the scope of a single paper. Therefore, our goals in this initial study are modest; we document the seasonally varying and site-specific cloud-layer overlap characteristics as a function of layer separation and compare these results to each other and to previous observational studies.

## 2. Data and technique

The 35-GHz millimeter cloud radars (MMCR; Moran et al. 1998) at the ARM central facilities (Table 1) are vertically pointing systems designed to map the distribution of clouds and precipitation in the vertical columns above the instruments. The MMCRs use relatively low peak-power transmitters (100 W), have a high duty cycle (25%), and have large antennas [57.2-dB gain at the Southern Great Plains (SGP) site and ~53 dB gain at the North Slope of Alaska (NSA) and the tropical western Pacific (TWP) sites] that allow for high sensitivity (near −50 dB$Z_e$ at 5 km). The sensitivity of the MMCR's over a wide range of cloud types is attributable to the design of the signal processing system where the radar is cycled through four distinct modes, each targeted to sense optimally a different class of hydrometeor. This observational approach is described fully in Clothiaux et al. (1999).

We combine the standard operational modes of the MMCR into a dataset with 90 m vertical and ~35 s temporal resolution to generate a binary description of significant echo return in the time-range domain of the data using a cloud masking algorithm similar to that described by Clothiaux et al. (1995). The masking algorithm is applied to each mode sequentially and the masks are then combined in a manner similar to that described by Clothiaux et al. (2000). Additionally, at the SGP site the sensitivity of the radar in the lower range gates often leads to significant return due to nonhydrometeor targets such as insects (we have found insect return to be a problem only at the SGP site and not at any of the other ARM sites). We, therefore, combine the radar mask with observations from collocated laser ceilometers to discriminate between cloud and other targets. This has the additional desired effect of discriminating between cloud and precipitation in the lowest hydrometeor layer since the laser instruments do not typically identify precipitation due to the generally low optical path associated with precipitation and due to tuning of the ceilometer algorithm thresholds.

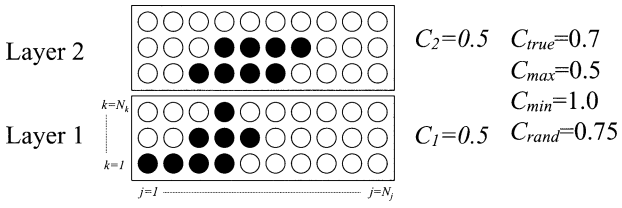


FIG. 1. A schematic illustration of Eqs. (1) and (2) for calculating cloud cover fraction and the various cloud overlap parameters discussed in the text. In the diagram, layers 1 and 2 refer to boxes representing some predetermined time (horizontal axis, $j$) and height (vertical axis, $k$) intervals. The circles within the boxes represent individual radar observations (nominally 35 s and 90 m, in our data). The open circles are meant to represent volumes with no significant radar return, while filled volumes are to represent volumes with hydrometeor occurrence. The coverage fraction of each box is 0.5 while the actual coverage fraction of the combined layers is 0.7. Of the standard assumptions, an assumption of random overlap comes closest to matching the actual cloud cover fraction in this example.

To evaluate cloud-layer overlap, we essentially follow the technique introduced by HI00. Our initial goal is to compare directly with their results so we use their temporal- and vertical-averaging interval for this purpose (1 h and 360 m). We also examine the overlap statistics at various temporal resolutions and also use the vertical grid of the National Center for Atmospheric Research (NCAR) Community Climate Model (CCM3; Kiehl et al. 1998) to examine the overlap characteristics in the vertical domain of a typical GCM. The cloud-masked radar data are collected into boxes with the appropriate time and height intervals. We will refer to these boxes as layers for a specific time interval. For each layer, we generate a simple cloud cover fraction, $C$, shown schematically in Fig. 1 and defined as

$$C = \frac{\sum_{j=0}^{N_j} i(j)}{N_j} \tag{1}$$

where

$$i(j) = 1; \quad \sum_{k=0}^{N_k} M_j(k) \neq 0, \quad \text{and}$$

$$i(j) = 0; \quad \sum_{k=0}^{N_k} M_j(k) = 0.$$

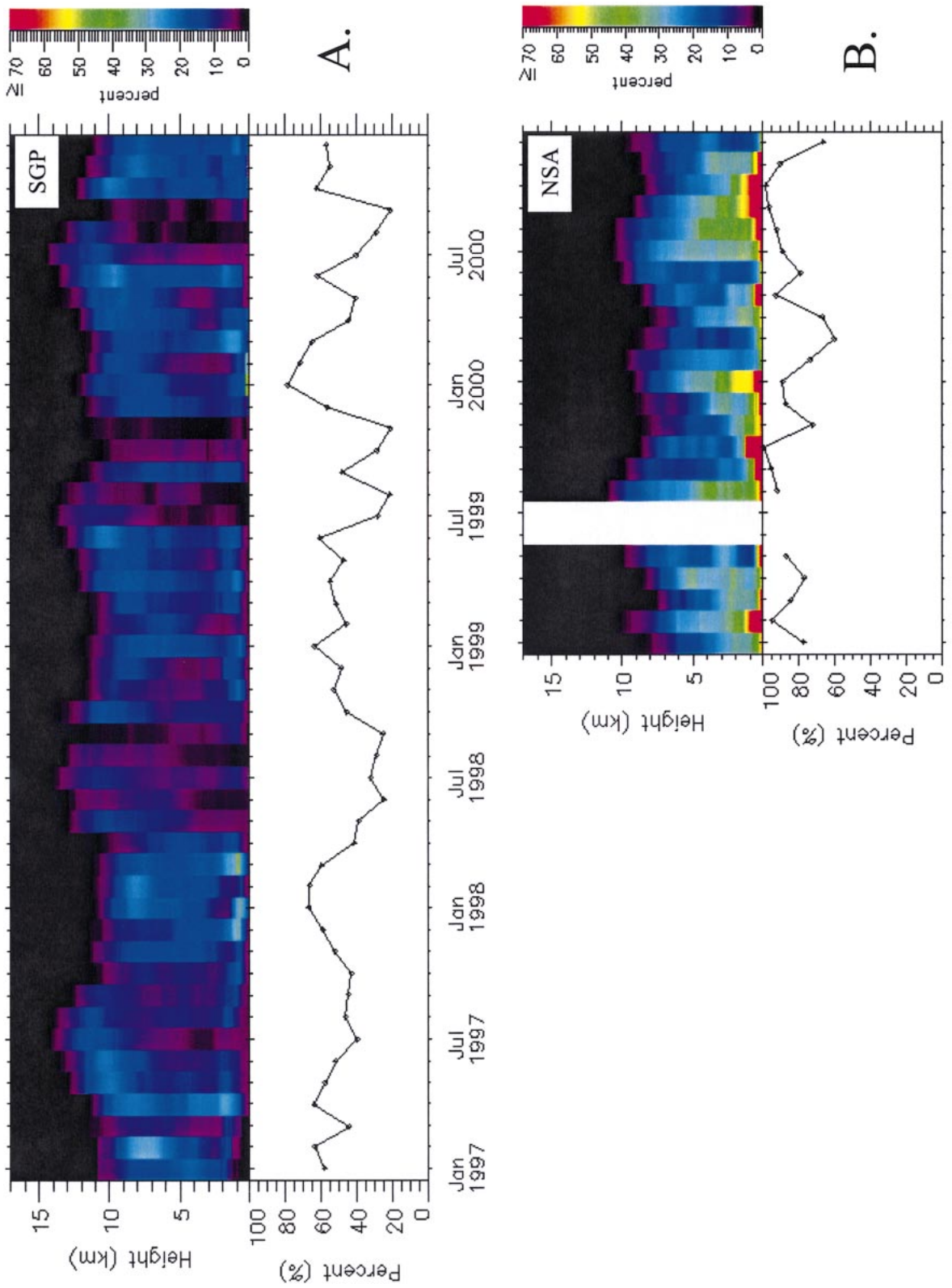


FIG. 2. Monthly averaged cloud fractions observed by the MMCR at the ARM sites. In each panel the top graphic shows the monthly cloud occurrence fraction in each 90-m range bin while the bottom panel shows the monthly mean hourly cloud coverage fraction: (a) SGP, (b) NSA, (c) TWP C1, (d) TWP C2.

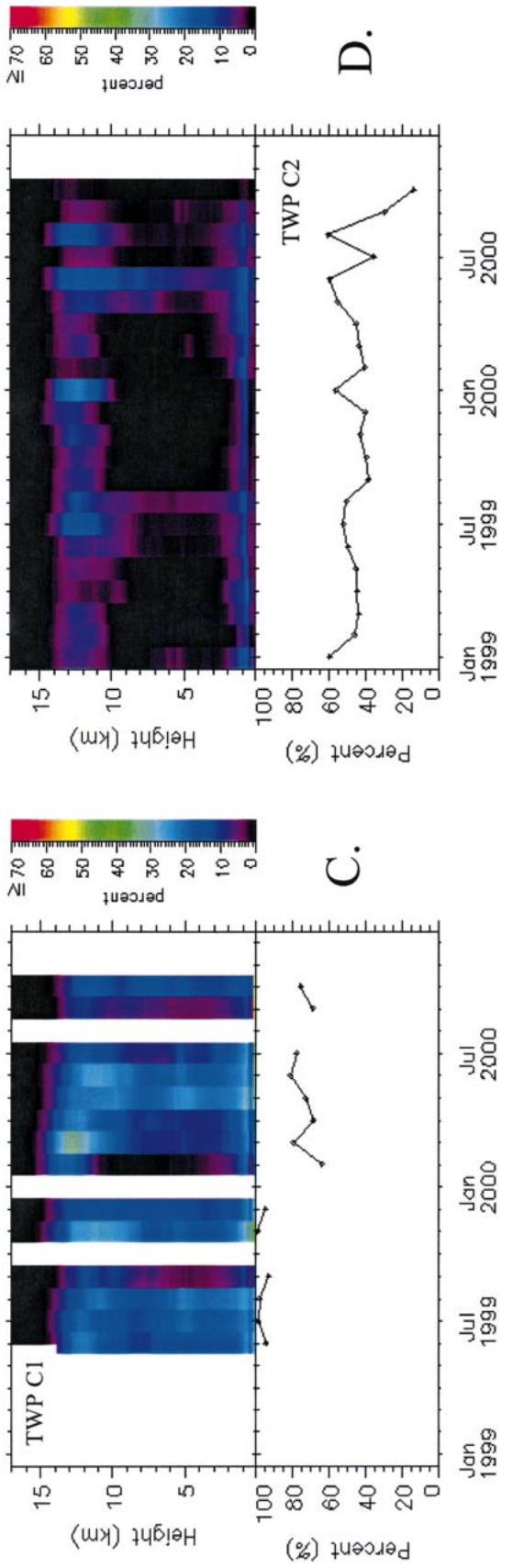


FIG. 2. (*Continued*)

Here, $M$ represents the original cloud mask, $j$ counts the number $N_j$ of 30-s time intervals in the layer, $k$ counts the number $N_k$ of 90-m height intervals, and $i$ records the presence of cloud in the vertical dimension of the layer at a specific time. The cloud cover as we define it here should be clearly distinguished from a volume cloud fraction, which would simply be the ratio of the number of hydrometeor occurrences in the layer divided by the total number of possible occurrences. Again, following HI00, to evaluate the cloud-layer overlap, the layers where $0 < C < 1$ at a specific time interval are analyzed in pairs, with every possible combination of layers considered (except for a layer compared to itself). The combined cloud fraction ($c_{\text{true}}$) of any two layers was calculated according to Eq. (1) where $N_k = 2$ and $M$ is replaced by $i$ for the two layers under consideration. In other words, $c_{\text{true}}$ is the cloud-cover fraction of the combined layers. The cloud covers, $C$, of any two layers was also used to calculate the values of the three standard overlap assumptions:

$$C_{\text{max}} = \max(C_1, C_2),$$
$$C_{\text{min}} = \min(1, C_1 + C_2), \quad \text{and}$$
$$C_{\text{rand}} = C_1 + C_2 - C_1C_2. \tag{2}$$

HI00 also introduce a straightforward technique to evaluate the degree to which $c_{\text{true}}$ agrees with any of the standard overlap assumptions:

$$c_{\text{true}} = \alpha C_{\text{max}} + (1 - \alpha)C_{\text{rand}}. \tag{3}$$

The value of $\alpha$, then effectively quantifies the agreement. When $\alpha = 0$, the overlap agrees with a random assumption, and when $\alpha = 1$ the overlap is maximal and the cloud-cover fraction is a minimum. As $c_{\text{true}}$ departs more and more from $C_{\text{max}}$ (trends toward $C_{\text{min}}$), $\alpha$ becomes negative.

Typically, parameterizations of overlap assume that layers separated by any clear layers can be considered randomly overlapped while layers separated by only cloud layers (i.e., vertically continuous cloud) are assumed to overlap maximally. We, therefore, generally separate our analysis similarly into layers with at least one intervening noncloudy ($C = 0.0$) layer and those layers separated by other cloud layers (i.e., vertically continuous cloud). The semantics here are important: we reserve the word ''layer'' to refer to a particular vertical resolution of a model or data instead of the usual terminology where a cloud layer refers to the entire vertical extent of the particular cloud.

## 3. Results

### *a. Cloud occurrence*

We present in Fig. 2 the monthly averaged cloud occurrence fractions in each 90-m-vertical range bin from the four sites. Also shown are monthly averaged, hourly mean coverage fractions, $C$, where Eq. (1) is applied so

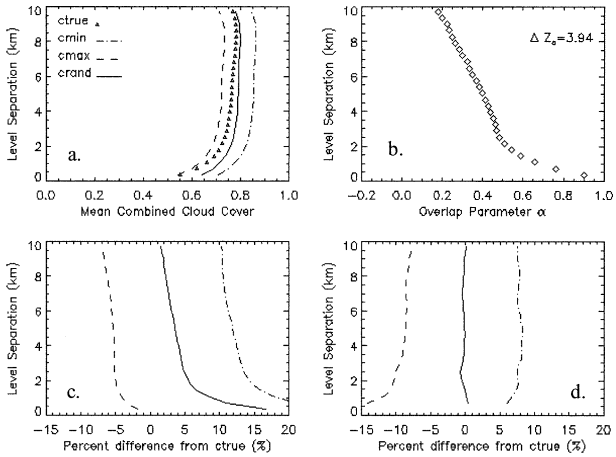


FIG. 3. Layer overlap statistics for the full SGP dataset averaged to 360 m and 1 h. (a) Actual and predicted mean cloud cover for cloudy layer pairs that compose parts of vertically contiguous cloudy layers. (b) The values of $\alpha$ [Eq. (2)] for the vertically continuous layer pairs along with an exponential fit to the results. The fit suggested by HI00 is shown for reference. (c) The percent error in cloud cover as a function of vertical separation for the vertically contiguous layers for the three standard overlap assumptions. (d) Same as in (c), except for layer pairs that are separated by noncloudy layers.

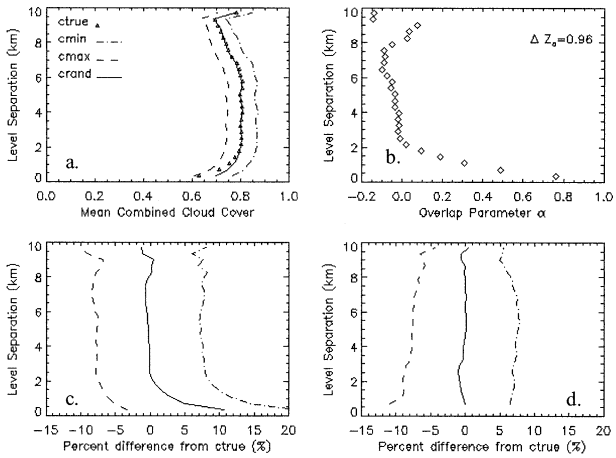


FIG. 4. As in Fig. 3, except for data collected at the NSA site during the period listed in Table 1.

that *j* extends over 1 h and *k* extends over the full vertical profile. The coverage is then averaged over each month. Even though the record is still relatively short at several of the sites, many interesting features that relate to the known cloud climatologies of these regions can be readily identified. The NSA time series, for instance, shows that cloud occurrence is predominantly weighted toward the lower troposphere with occurrence peaks in late summer and early autumn in agreement with what has been reported elsewhere (Curry et al. 2000). Minima in cloud occurrence are observed in winter and early spring of this relatively short record. While we find occurrence peaks of more than 70% in individual range gates during certain periods at NSA, the hourly averaged coverage fraction is more than 80% during most months and reaches nearly 100% during autumn 2000.

The SGP time series reveals a distinct seasonal deepening of the troposphere during summer. Cloud occurrence appears to be minimal during the late summer at this site and reaches a peak during the late autumn and winter when synoptic-scale weather systems are most active. During the spring and summer months at SGP, boundary layer clouds and cirrus appear to be predominant cloud types, while reasonably distinct minima in cloud occurrences are observed in the middle troposphere during these seasons (e.g., Uttal et al. 1995; Lazarus et al. 2000). The SGP record is long enough that we are able to qualitatively compare seasons and even annual cycles. For instance, we find that the summer months of 1997 appear to be the most cloudy of the four summer seasons documented here while the summer or 1998 appears to be consistently the least cloudy due primarily to a deficit (compared to other years) of boundary layer clouds during that period.

The tropical sites show distinct differences from one another that are representative of their longitudinal positioning along the so-called Walker circulation (Rosenlof et al. 1986; see Table 1). During this period, also, a major La Niña cycle likely magnified the differences between the two locales. The most striking differences are related to the more extensive cloud occurrence through the middle troposphere at the Manus Island site (TWP C1) compared to Nauru Island (TWP C2) in the monthly means. Inspection of the data suggests that much of this cloud occurrence in the middle troposphere at Manus Island is due to more frequent and deeper cumulus convection than is observed at Nauru during this time. Cloud cover over Nauru in 1999 and 2000 appears to be predominantly composed of cirrus and boundary layer cloud. We should note that the boundary layer cloud that appears in this record at Nauru, might not be entirely representative of the open ocean region surrounding the island due to an island-generated cumulus cloud street that biases this record and is most predominant during periods when deep cumulus convection is largely suppressed.

### *b. Cloud overlap—Geographic sensitivity*

We begin with a discussion of the cloud-layer overlap characteristics of the full datasets from each site segregated into two classes: vertically continuous layers and layers with intervening clear layers. We then examine the sensitivity of the overlap assumption as it pertains to seasonal differences at the sites and the sensitivity to temporal and vertical resolution. Figures 3–6 show the cloud overlap statistics compiled from the data presented in Fig. 2. Since we use a vertical and temporal resolution identical to that used by HI00, these results can be compared directly to their Figs. 3 and 4. HI00 found that cloudy layers separated by clear layers

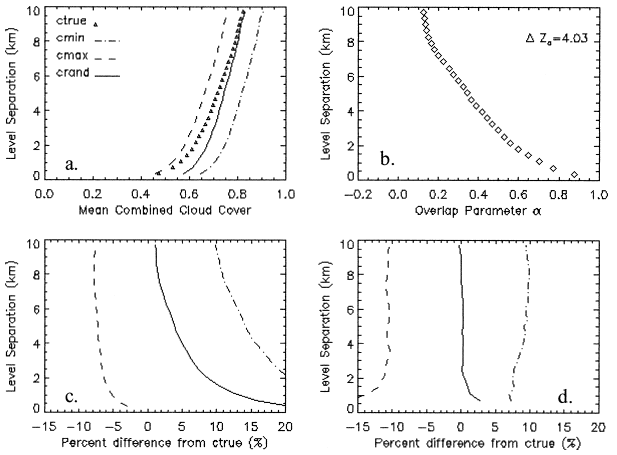


FIG. 5. As in Fig. 3, except for data collected at the TWP C1 site (Manus Island) during the period listed in Table 1.

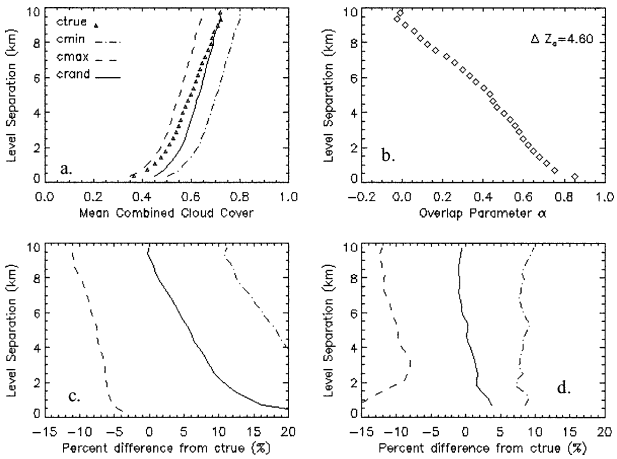


FIG. 6. As in Fig. 3, except for data collected at the TWP C2 site (Nauru Island) during the period listed in Table 1.

could be considered randomly overlapped. Our results (Figs. 3d, 4d, 5d, 6d) at all sites show the same tendency with slight deviations that result in insignificant biases when considering the full datasets. For instance at Nauru (TWP C2), an assumption of random overlap would lead to a positive bias in cloud cover predictions for layers separated by less than 3–4 km. The data suggest a tendency toward maximum overlap, while for layers separated by more than approximately 6 km, the bias becomes slightly negative suggesting a slight trend toward minimal overlap. These trends, not seen in the Manus Island data, may be related to the tendency for the island-generated cumulus to be less prominent during periods when nearby convection is generating cirrus. In other words, a reduction in downwelling solar radiation in the presence of higher, thicker clouds may suppress the formation of the island-generated cumulus. At other sites, both NSA and TWP C2 show a slight trend toward minimum overlap for noncontiguous layers separated by approximately 2 km. While these tendencies appear irrelevant in this broad view, they may be statistically meaningful for certain synoptic conditions where correctly characterizing the layer overlap could lead to substantially different and arguably more correct predictions of the area-averaged radiation budget. This issue requires further analysis where the overlap is examined in terms of objectively classified synoptic type (Lau and Crane 1995).

When considering the overlap characteristics of vertically contiguous layers, most radiation transfer schemes in general circulation models (GCMs) assume such layers are maximally overlapped resulting in minimal total cloud cover. Barker et al. (1999) found using output from a cloud resolving model (CRM) run for a tropical case that this assumption results in too little cloud cover compared to the actual cloud fraction in the CRM domain. In apparent agreement with the CRM results, HI00, using data collected during winter in southern England, show a strong tendency for vertically contiguous cloud layers to be randomly overlapped when the layer separation increases much beyond a few kilometers. HI00 parameterized the tendency in $\alpha$ with a decaying exponential function and reported an *e*-folding height scale, $\Delta z_0$. This height scale was shown to be a strong function of the vertical and temporal resolution of the radar data (see Table 1 of HI00). Figs 4a–c show that the data collected at the NSA site agree well with the results of HI00. The layer overlap trends rapidly toward randomness with vertical separation. By 2 km of separation, the overlap characteristic of the layers is nearly purely random with some tendency toward minimum overlap for layers separated by 6–7 km. We find a separation distance scale, $\Delta z_0$, of approximately 1 km in the NSA data. Since the resolution of the data analyzed here is 360 m, the precision of $\Delta z_0$ derived from the NSA data is not high. The qualitative tendency toward random cloud overlap at this site is the important point, however.

This tendency toward randomly overlapped layers, however, is not found to be as strong in the cloud layers observed at the other ARM sites. Both Nauru and Manus Islands results demonstrate a tendency for layers to become randomly overlapped with increasing vertical separation but slowly, relative to the Point Barrow (NSA) and the Chilbolton data of HI00. A parameterization of $\alpha$ at the TWP sites would best be accomplished as a linear function of separation instead of with an exponential fit. The SGP data also show a tendency to slowly vary from maximum to random overlap but not quite so monotonically as the TWP sites. An evident scale break is seen in the SGP data near approximately 2-km separation. Below 2-km separation, the trend toward random overlap appears to be rapid while the trend is much less rapid for separations greater than 4 km, and appears to approach random overlap very nearly linearly with layer separation similar to the TWP data.

Based on this analysis, both the random and maximum overlap assumptions lead to substantial bias errors

TABLE 2. Approximate sigma, pressure and physical heights of the CCM3 vertical coordinates used to examine the overlap characteristics at SGP. The values of the other sites differed slightly.

| Sigma | Mean pressure (mb) | Mean height (km) |
|---|---|---|
| 0.138 | 135 | 15.0 |
| 0.189 | 185 | 13.1 |
| 0.251 | 245 | 11.4 |
| 0.32 | 317 | 9.6 |
| 0.41 | 398 | 7.9 |
| 0.50 | 489 | 6.4 |
| 0.59 | 584 | 5.1 |
| 0.69 | 678 | 3.8 |
| 0.78 | 767 | 2.7 |
| 0.87 | 845 | 1.9 |
| 0.93 | 906 | 1.2 |
| 0.97 | 946 | 0.7 |
| 0.99 | 968 | 0.5 |

of at least 4%–6% in fractional cloud cover for layers with 2–4 km vertical separation at the tropical and midlatitude observing sites (e.g., see Fig. 4). While these error values seem small, they are bias errors nonetheless and would, if applied over a wide region, induce a substantial bias error in the radiation budget (Barker et al. 1999). To put these errors into perspective we should also recall the oft quoted finding that a 4% increase in low cloud cover would be sufficient to offset the warming effect of a doubling of $CO_2$ (Randall et al. 1984). Therefore, these bias errors in cloud cover, if codified in GCMs, could mask or bias climate feedbacks resulting from increasing trace gasses or natural variability.

### c. *Cloud overlap—Sensitivity to vertical and temporal resolution*

To demonstrate the response of the overlap characteristics in the vertical scale of a GCM, we approximate the vertical grid of the CCM3 (Table 2) and examine the overlap characteristics for various temporal averaging times. The overall results do not differ qualitatively from those presented for 360-m averaging and are presented in Table 3 as CCM3, the second row of layer separation–scale distances $\Delta z_0$, except the units are now model layers instead of kilometers. The change in the $\Delta z_0$ parameter with decreasing temporal resolution is not, however, consistent across the ARM sites.

HI00 show that $\Delta z_0$ is quite sensitive to vertical and temporal resolution. The $\Delta z_0$ increased in their study as the vertical and temporal resolution of the radar cloud mask was reduced. In other words, with reduced resolution they found a tendency for the layer overlap characteristics of vertically contiguous layers to become less random. Our data (Table 3) show a similar tendency at the TWP sites but an opposite tendency at SGP, while the NSA data shows little significant trend. Several plausible arguments can be offered to explain these observations. As the effective spatial scale is increased by averaging the time series data over a longer period, one possible outcome would be for the overlap to trend toward increasing cloud cover (decreasing $\alpha$) as uncorrelated cloud features become grouped into the same time bin. Along the same line of reasoning, increasing the averaging period would lead to cloud features associated with vertical wind shears that are sloped in space to become more grouped together, maximizing the cloud cover between layers and leading to a potential reduction in $\alpha$. On the other hand, as put forth by HI00, decreasing the resolution would also tend to minimize the combined cloud cover simply by extending the averaging period over longer times. A pair of layers that have a coverage fraction of some value at a particular temporal resolution could only have less coverage as the resolution decreases. Examination of Eq. (3) shows that $\partial\alpha/\partial C_{\text{true}} = -1/(C_{\text{rand}} - C_{\text{max}})$, and since the denominator on the right can never be less than zero, $\alpha$ will tend to decrease as $C_{\text{true}}$ increases. This assumes, of course, that no other cloud elements are incorporated into the averaging period as it becomes longer. Evidently, this effect is predominant in the data collected at the tropical sites and in the data analyzed by HI00, but not at SGP. As averaging time is increased from 20 min to 2 h, we find the separation scale distance decreases by about a factor of 2. This characteristic appears to be insensitive to season, as shown in Table 4. In other

TABLE 3. Values of $\Delta z_0$ (separation distance scale) for the four ARM sites for various temporal averaging and at vertical resolutions of 360 m and the CCM3 sigma levels. Note the two rows of each site are different units.

| | Averaging period | | |
|---|---|---|---|
| Vertical resolution | 20 min | 1 h | 2 h |
| SGP | | | |
| 360 m (km) | 6.9 | 3.9 | 3.3 |
| CCM3 (layers) | 6.5 | 3.8 | 3.1 |
| NSA | | | |
| 360 m (km) | 0.8 | 1.0 | 1.1 |
| CCM3 (layers) | 0.9 | 0.9 | 0.9 |
| TWP C1 (Manus) | | | |
| 360 m (km) | 3.6 | 4.0 | 4.7 |
| CCM3 (layers) | 2.1 | 2.4 | 2.6 |
| TWP C2 (Nauru) | | | |
| 360 m (km) | 3.9 | 4.6 | 4.9 |
| CCM3 (layers) | 2.2 | 2.7 | 2.7 |

TABLE 4. Values of $\Delta z_0$ at SGP for the CCM3 vertical grid as a function of season for various averaging times. Here we define the warm season to be May, Jun, Jul, and Aug and the cold season to be Nov, Dec, Jan, and Feb. The units of the values here are CCM3 layers.

| | Season averaging period | | |
|---|---|---|---|
| CCM3 (layers) | 20 min | 1 h | 2 h |
| SGP (cold) | 3.1 | 1.7 | 1.4 |
| SGP (warm) | 8.7 | 5.1 | 4.1 |

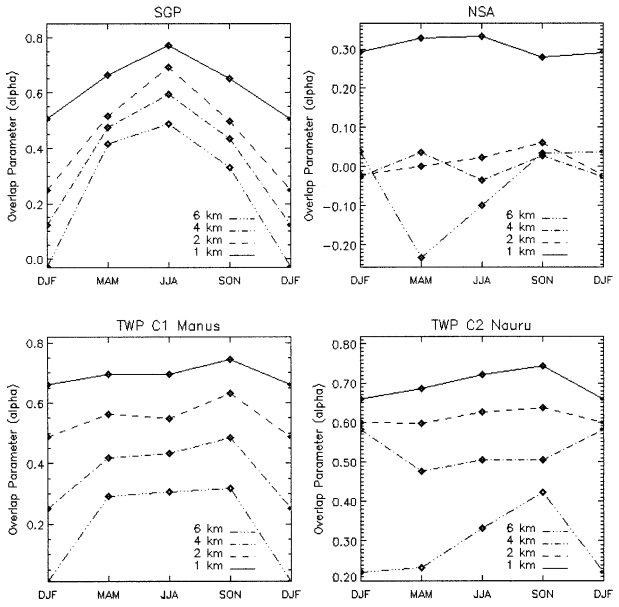


FIG. 7. Composite annual cycle of the overlap parameter $\alpha$ for vertically contiguous layers at the four ARM sites for various layer separations. The overlap characteristics were evaluated for all observations within a particular 3-month period. Note from Table 1 that the SGP record (47 months) is substantially longer than all the other sites, while TWP C1 is only 14 months.

words, the tendency is for the cloud layers at SGP to become more randomly overlapped as the averaging time is increased. Interestingly we can see a very strong dependence of the magnitude of $\Delta z_0$ on the time of year; the degree of randomness in the cloud-layer overlap is substantially greater during the cold season, as one would expect if cloud systems are driven by processes related to convection during the warm season and synoptic scale systems during winter. We examine this finding in more detail in the following section.

### *d. Overlap sensitivity to season*

We have shown thus far that the overlap characteristics depend strongly on the geographic location, the vertical and temporal resolution of the data, and as Table 4 suggests, somewhat on the season. To further explore the seasonal dependencies, Fig. 7 shows $\alpha$ for composite annual cycles at the four ARM sites. To produce Fig. 7, the 360-m and 1-h temporal resolution was used and $\alpha$, calculated for all cloud layers observed during a particular season, is plotted for various layer separations. Some care should be taken interpreting this figure since different observational record lengths are used to generate the results (Table 1). SGP with 4 annual cycles has the most extensive record, while the other sites have from 1.5 to 2 annual cycles. We find that SGP shows a rather striking annual cycle where the overlap parameter, $\alpha$, varies quite substantially at all levels. During the summer season, an assumption of maximal overlap for vertically contiguous layers causes less error in cloud cover than during the winter season when the overlap characteristics are much more random and thus result in greater overall cloud cover. The other sites, however, show much less seasonality in the layer overlap characteristics. At NSA, an assumption of random overlap for contiguous layers separated by more than 1–2 km is a very good assumption, implying that the standard assumption of maximal overlap for vertically contiguous layers significantly biases cloud cover estimates lower than the actual amount. The TWP sites are similar to one another and also show no seasonality in the overlap characteristics for these relatively short data records.

Finally in Fig. 8, we consider the seasonal time series of the $\alpha$ parameter at SGP. The annual cycle is clearly discernible in this time series as is some variability between years and individual seasons. Overall, the overlap characteristics are somewhat more maximal during 1997 and 1998 compared to 1999 and 2000. This tendency

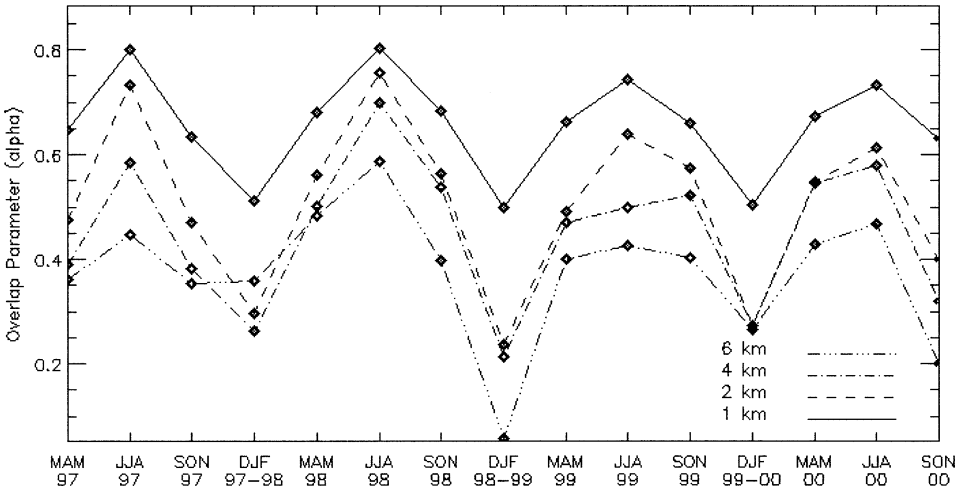


FIG. 8. Seasonal time series of the overlap parameter $\alpha$ for vertically contiguous layers at SGP.

is mostly seen in the warm season months while the winter months are somewhat similar to one another with the exception of December–January–February (DJF) 1989–99. During DJF 1998–99, we find that layers separated by 1 km have similar characteristics to other winters. However, for layer separations more than 1 km, the overlap characteristics appear significantly more random than other years.

## 4. Summary and conclusions

We have presented an initial evaluation of cloud-layer overlap characteristics derived from millimeter cloud radar data collected at the four ARM central facilities (Table 1). This dataset documents the cloud-layer overlap characteristics of substantially different climatic regimes (deep Tropics to the Arctic) and extends over sufficient time to characterize seasonal variability in cloudiness. Prior studies have used satellite data (TC89), cloud radar data of shorter duration (HI00) or model output (Barker et al. 1999). The results presented herein confirm some previous findings although these results also call into question certain other long-held assumptions. The primary findings of this study are the following.

1) In agreement with standard assumptions (Geleyn and Hollingsworth 1979), the overlap characteristics of cloudy layers that are separated by clear layers can be treated as randomly overlapped. This result appears to hold on average at all sites regardless of the temporal resolution considered. Additional work should, however, explore the possibility that different overlap characteristics are applicable for certain synoptic conditions even for these types of layers.
2) With the exception of cloudiness observed at the NSA location, the overlap characteristics of cloud layers that are parts of vertically contiguous cloudy layers do not, in general, lend themselves to a simple overlap assumption of either random or maximum. This result is counter to the widely applied assumption that vertically contiguous layers are maximally overlapped (Geleyn and Hollingsworth 1979). We find that on average at the SGP and the TWP sites, the layer overlap trends slowly from maximal for closely spaced layers (less than 1 km) to random for layers separated many ($>6$) kilometers. Between these extremes, the overlap characteristics appear to change gradually. Cloudiness observed at the NSA location, like the data analyzed by HI00, show that at these locations any layers separated by much more than 1 km can be modeled as randomly overlapped.
3) The SGP site demonstrates a well-defined seasonal cycle in the cloud-layer overlap characteristics of vertically contiguous layers. This suggests that a single assumption of cloud overlap at this middle-latitude site will be wrong at least some of the time. However this result also strongly implies that the synoptic setting or the cloud formation mechanism could be used as a means to parameterize the overlap characteristics in numerical models. No seasonal dependence was found in the layer overlap characteristics at the other ARM sites although the data record at the other sites was substantially shorter.

These findings call into serious question the way clouds are represented in most GCMs. If our conclusions can be generally applied, for a GCM to agree with Earth Radiation Budget Experiment (ERBE) top-of-atmosphere fluxes while biasing the overall cloud cover low suggests that the radiative properties of the clouds would be incorrect and likely biased toward too much extinction. This will result an incorrect vertical distribution of heating in the column and ultimately influence improperly the predicted atmospheric circulation and surface energy budget.

While this study significantly extends the volume of data used to examine the cloud-layer overlap problem, these results should still be considered somewhat preliminary. One of the questions that future work must address is how relevant are time-averaged point data to grid-box mean values? While some preliminary evidence exists to suggest that the connection between time and space can be made, a more thorough examination of this issue is needed. A corollary to the time–space problem is the relevance of a given location to broader regional statistics. How relevant is the SGP record to, for instance, the northern middle latitudes in general? Since the SGP site exists in a rather unique location with the Gulf of Mexico to the south, source regions of arctic air to the north, and a substantial mountain range to the west, applying lessons learned from the statistics acquired at SGP to broader geographic regions would at least require validation (1–2 annual cycles of cloud radar data) from other locations. Therefore, either additional long-term sites are necessary or an observational methodology is needed to fill in the substantial gaps in the present observational record. Certainly space-based cloud radar (Stephens et al. 2001 manuscript submitted to *Bull. Amer. Meteor. Soc.*) will prove an indispensable tool in this regard and will partially fill the spatial gaps left by the ground-based network. Since Cloudsat (95-GHz cloud radar that is scheduled for launch in 2004) will be sun synchronous and vertically pointing, the space-based radar data will be complementary to the operational ground-based network, and their combination will provide a dataset sufficient to more thoroughly address this important problem.

*Acknowledgments.* Funding for this work was provided by the Environmental Science Division of the U.S. Department of Energy (Grant DE-FG0398ER62571) and through a NASA EOS Validation Program grant (NAG56458). Data were obtained from the Atmospheric Radiation Measurement Program sponsored by the U.S. Department of Energy, Office of Science, Office of Bi-

ological and Environmental Research, Environmental Sciences Division.

## REFERENCES


Barker, H. W., G. L. Stephens, and Q. Fu., 1999: The sensitivity of domain-averaged solar fluxes to assumptions about cloud geometry. *Quart. J. Roy. Meteor. Soc.,* **125,** 2127–2152.

Barnett, T. P., J. Ritchie, J. Float, and G. Stokes, 1998: On the space–time scales of the surface solar radiation field. *J. Climate,* **11,** 88–96.

Clothiaux, E. E., M. A. Miller, B. A. Albrecht, T. P. Ackerman, J. Verlinde, D. M. Babb, R. M. Peters, and W. J. Syrett, 1995: An evaluation of a 94-GHz radar for remote sensing of cloud properties. *J. Atmos. Oceanic Technol.,* **12,** 201–229.

——, and Coauthors, 1999: The Atmospheric Radiation Measurement Program cloud radars: Operational modes. *J. Atmos. Oceanic Technol.,* **16,** 819–827.

——, T. P. Ackerman, G. G. Mace, K. P. Moran, R. T. Marchand, M. A. Miller, and B. E. Martner, 2000: Objective determination of cloud heights and radar reflectivities using a combination of active remote sensors at the ARM CART sites. *J. Appl. Meteor.,* **39,** 645–665.

Curry, J. A., and Coauthors, 2000: FIRE Arctic Clouds Experiment. *Bull. Amer. Meteor. Soc.,* **81,** 5–29.

Fye, F. K., 1978: The AFGWC automated cloud analysis model. Offutt Air Force Base U.S. Air Force Global Weather Central, Tech. Memo. 78-002.

Geleyn, J. F., and A. Hollingsworth, 1979: An economical analytical method for the computation of the interaction between scatering and lin absorption of radiation. *Contrib. Atmos. Phys.,* **52,** 1–16.

Hahn, C. J., S. G. Warren, J. London, R. M. Chervin, and R. Jenne, 1982: Atlas of simultaneous occurrence of different cloud types over the ocean. NCAR Tech. Note TN-201+STR NCAR, 212 pp.

Hogan, R. J., and A. J. Illingworth, 2000: Deriving cloud overlap statistics from radar. *Quart. J. Roy. Meteor. Soc.,* **126,** 2903–2909.

Houghton, J. T., G. L. Jenkins, and J. J. Ephraums, Eds.,1990: *Scientific Assessment of Climate Change—Report of Working Group I.* Cambridge University Press, 365 pp.

Jakob, C., and S. A. Klein, 1999: A parameterization of the effects of cloud and precipitation overlap for use in general circulation models. *Quart. J. Roy. Meteor. Soc.,* **126,** 2525–2544.

Kiehl, J. T., J. J. Hack, G. B. Bonan, B. A. Boville, D. L. Williamson, and P. J. Rasch, 1998: The National Center for Atmospheric Research Community Climate Model: CCM3. *J. Climate,* **11,** 1131–1149.

Kropfli, R. A., and Coauthors, 1995: Cloud physics studies with 8-mm wavelength radar. *Atmos. Res.,* **35,** 299–313.

Lau, N.-C., and M. W. Crane, 1995: A satellite view of the synoptic-scale organization of cloud properties in midlatitude and tropical circulation systems. *Mon. Wea. Rev.,* **123,** 1984–2006.

Lazarus, S. M., S. K. Krueger, and G. G. Mace, 2000: A cloud climatology of the Southern Great Plains ARM CART. *J. Climate,* **13,** 1762–1775.

Long, C. N., and T. P. Ackerman, 1995: Surface measurements of solar irradiance: A study of the spatial correlation between simultaneous measurements at separated sites. *J. Appl. Meteor.,* **34,** 1039–1046.

Mace, G. G., C. Jakob, and K. P. Moran, 1998: Validation of hydrometeor prediction from the ECMWF model during winter season 1997 using millimeter wave radar data. *Geophys. Res. Lett.,* **25,** 1645–1648.

Moran, K. P., B. E. Marner, M. J. Post, R. A. Kropfli, D. C. Welsh, and K. B. Widener, 1998: An unattended cloud-profiling radar for use in climate research. *Bull. Amer. Meteor. Soc.,* **79,** 443–455.

Morcrette, J., and C. Jakob, 2000: The response of the ECMWF model to changes in the cloud overlap assumption. *Mon. Wea. Rev.,* **128,** 1707–1732.

Randall, D. A., J. A. Coakley, C. W. Fairall, R. A. Kropfli, and D. H. Lenschow, 1984: Outlook for research on subtropical marine stratiform clouds. *Bull. Amer. Meteor. Soc.,* **65,** 1290–1301.

Rosenlof, K. H., D. E. Stevens, J. R. Anderson, and P. E. Ciesielski, 1986: The Walker Circulation with observed zonal winds, a mean Hadley cell, and cumulus friction. *J. Atmos. Sci.,* **43,** 449–467.

Slingo, J. M., 1987: The development and verification of a cloud prediction scheme for the ECMWF model. *Quart. J. Roy. Meteor. Soc.,* **113,** 899–927.

Stokes, G. M., and S. E. Schwartz, 1994: The Atmospheric Radiation Measurement (ARM) Program: Programmatic background and design of the cloud and radiation test bed. *Bull. Amer. Meteor. Soc.,* **75,** 1201–1221.

Tian, L., and J. A. Curry, 1989: Cloud overlap statistics. *J. Geophys. Res.,* **94,** 9925–9935.

Uttal, T., E. E. Clothiaux, T. P. Ackerman, J. M. Intrieri, and W. L. Eberhard, 1995: Cloud boundary statistics during FIRE II. *J. Atmos. Sci.,* **52,** 4276–4284.

Warren, S. G., C. J. Hahn, J. London, R. M. Chervin, and R. L. Jenne, 1986: Global distribution of total cloud cover and cloud type amounts over land. NCAR Tech. Note NCAR/TN-273+STR, 231 pp.

Wetherald, R. T., and S. Manabe, 1988: Cloud feedback processes in a general circulation model. *J. Atmos. Sci.,* **45,** 1397–1415.

Yao, M.-S., and A. D. Del Genio, 1999: Effects of cloud parameterization on the simulation of climate changes in the GISS GCM. *J. Climate.,* **12,** 761–779.